

GUGGENHEIM AERONAUTICAL LABORATORY

CALIFORNIA INSTITUTE OF TECHNOLOGY

STABILIZATION OF A BI-PROPELLANT LIQUID ROCKET MOTOR

Thesis by

Dale W. Cox, Jr.
LCDR USN

PASADENA, CALIFORNIA

THESIS
C757

Library
U. S. Naval Postgraduate School
Monterey, California

STABILIZATION OF A BI-PROPELLANT LIQUID ROCKET MOTOR

Thesis by

LCDR Dale W. Cox, Jr., USN

In Partial Fulfillment of the Requirements

For the Degree of

Aeronautical Engineer

California Institute of Technology

Pasadena, California

1952

ACKNOWLEDGMENT

The author is indebted to Dr. Frank E. Marble and Dr. H. S. Tsien, both of the Jet Propulsion Center, California Institute of Technology, for their help and guidance in this problem.

SUMMARY

The unstable burning of a bipropellant rocket combustion chamber is investigated and a study made of the requirements for an automatic closed loop control circuit to stabilize the motor.

The bipropellant combustion chamber equations developed by Dr. L. Crocco⁽¹⁾ are utilized as the analytical description of the rocket motor burning phenomena. Equations similar to those developed by Dr. H. S. Tsien⁽²⁾ are used for the oxidizer and fuel supply systems and the two closed loop stabilizing circuits.

The stability or instability of the system is demonstrated by the use of a special plotting diagram in the complex plane suggested by H. Satche as a means of handling systems with time lag, and developed for this use by H. S. Tsien. This involves separating the transfer function into two parts. In the complex plane the first portion of the transfer function, the exponential variable containing the time lag, plots as a unit circle as the complex variable p is made to take a contour enclosing the positive half of the p -plane. If the remaining portion of the transfer function intersects this unit circle, the rocket motor can be unstable for large reduced time lag; if it does not intersect the unit circle, the system is generally stable, although the roots of the exponential coefficient in the positive half of the complex plane must be investigated. This

latter requirement can be conveniently accomplished by the aid of a Nyquist Diagram.

The equations for the feedback circuit are developed and the oxidizer and fuel transfer function requirements are determined.

Two cases of stable combustion and two cases of unstable combustion are analyzed. One unstable case is stabilized by the addition of a feedback circuit.

TABLE OF CONTENTS

PART	TITLE	PAGE
	Acknowledgement	i
	Summary	ii
	Table of Contents	iv
	Symbols and Definitions	v
I	Introduction	1
II	Development of Equations	5
III	Stability of Bipropellant Systems Without Feedback	12
IV	Stabilization of a Bipropellant System by a Feedback Circuit	17
	References	25
	Graphs for Cases Considered	

SYMBOLS AND DEFINITIONS

t	=	time
τ	=	instantaneous value of the time lag
n	=	pressure exponent of pressure dependence of the processes taking place during the time lag
p	=	instantaneous pressure in the combustion chamber
also, p	=	$\lambda + i\omega$ = root of the characteristic equation with the reduced time as the independent variable
\bar{p}	=	pressure in the combustion chamber in steady operation
ϕ	=	$(p - \bar{p})/\bar{p}$ = fractional variation of pressure in the combustion chamber
$\dot{m}_1, \dot{m}_b, \dot{m}_e$	=	instantaneous rate of injection, burning, and ejection of propellants
$\bar{\dot{m}}$	=	common value of the above rates of injection, burning and ejection in steady operation
μ	=	$(\dot{m}_1 - \bar{\dot{m}})/\bar{\dot{m}}$ = fractional variation of injection rate
M_g	=	instantaneous mass of gases in the combustion chamber
θ_g	=	$M_g/\bar{\dot{m}}$ = gas residence time in steady operation
θ_t	=	$\theta_g + \tau$ = total residence time of propellants in steady operation
T_g	=	absolute temperature of combustion gases

λ	=	reduced amplification coefficient
ω	=	reduced angular frequency
r	=	instantaneous mixture ratio
\bar{r}	=	mixture ratio in steady operation
K	=	coefficient related to the variation of temperature with mixture ratio
K_o	=	non-dimensional reservoir capacity for the oxidizer line
K_f	=	non-dimensional reservoir capacity for the fuel line
R	=	$(\bar{r} - 1) / 2 (\bar{r} + 1)$ = coefficient representing the deviation from unity of the mixture ratio
i	=	subscript indicating injector end
e	=	subscript indicating ejector end
o	=	subscript indicating oxidizer
f	=	subscript indicating fuel
z	=	t / θ_g = reduced time
δ	=	$\bar{\tau} / \theta_g$ = reduced time lag
α	=	constant relating the mass flow rate to the pressure in the feed system lines
J	=	$\bar{\Delta} / 2 \Delta p A_t \theta_g$ = inertia parameter in the line
P	=	$\bar{p} / 2 \Delta p$ = pressure drop parameter
F_o, F_f	=	ratio of functions in (d/dz) describing the response of the feedback circuits
g	=	$H + 2K - K e^{-P}$ = a convenient grouping of terms

A', B', D', L', M'	=	complex constants used in the trial solution
$G(p)$	=	system transfer function
$g_1(p), g_2(p)$	=	components of $G(p)$ used in the Tsien-Satche Diagram
A, C, D, R, S	=	convenient system constants defined in equations (16) through (21)
L, M	=	convenient grouping of system constants and variables defined in equations (22) and (23)
Ψ	=	$F_0(p)L - F_f(p)M = a_{-1}/p + a_0 + a_1 + a_2$ a convenient symbol for the feedback circuit's transfer function

I. INTRODUCTION

Rocket motors often exhibit rough combustion either as chugging (low frequency oscillation below 100 cycles per second) or screaming (high frequency oscillations several hundreds of cycles per second). The first of these phenomena has been investigated sufficiently that several authors have developed equations describing analytically the oscillation processes in rocket motors⁽¹⁾. Those equations which are utilized in this paper are deduced by L. Crocco under the following assumptions:

1. The processes of transforming the propellants into high temperature gases require a certain time called the time lag, τ ; it is the time after which the liquids may be considered suddenly transformed into hot gases. The rate of mixing of the propellants depends essentially on the injection system used and recirculation effects, but probably not on chamber pressure. The conditions, droplet size, temperature, vaporization and eventual chemical transformation of the propellants after mixing depend considerably on chamber pressure.
2. The time lag is considered the same for all particles of the propellants; the residence time is considered the same for all particles, i.e., all particles travel from the injector end where burning occurs to the exhaust end in the same residence time interval.

3. The law of variation of time lag with pressure is assumed to be:

$$\int_{t-\tau}^t f(p) dt' = \text{constant} \quad (1)$$

where p is the chamber pressure and $f(p)$ is the time rate of preparation for combustion.

4. Pressure variations are sufficiently slow throughout the combustion chamber that a uniform pressure can be used, $p = p(t)$.

5. Temperature of the gases is assumed to vary with time and space but not with pressure oscillations.

6. Analysis of the stabilizing circuit itself and its oscillations affecting the rocket motor are not investigated.

L. Crocco⁽¹⁾ has demonstrated that a rocket combustion chamber is intrinsically unstable, i.e., the burning phenomena itself can generate oscillations even without variation in the injection rate. This occurs because any oscillations of the pressure will cause an oscillation in the time lag by equation (1). Thus if the time lag is oscillating, it is immediately seen that when the time lag is decreasing, the burning of the particles that were injected later will catch up with the burning of those injected earlier; this increases the rate of burning with respect to the average. Similarly, the opposite happens for an increasing time lag. Thus, if the increased or decreased rate of burning should coincide with a pressure

increase or decrease, self-excited oscillations can exist resulting in unstable burning.

For the bipropellant case assumption 2 that Θ_g is the residence time of all particles means that each particle burns at the injector end and travels to the exhaust end carrying with it the temperature developed at the combustion instant. Thus, the temperature at the exhaust, T_{ge} , at the time t corresponds to the mixture ratio of the propellants injected at the earlier time $t - \Theta_g = t - \tau - \Theta_g$. This can be put in terms of the reduced time by dividing by Θ_g giving: $z - \delta - 1$. Therefore, in effect, we have two reduced time lags, δ and 1.0. It is the second time lag that introduces additional complications in the formulas for the bipropellant case by appearing as an exponential term in $g_2(p)$.

The problem of stabilizing a combustion chamber is simplified by the use of the Tsien-Satche Diagram. If the system transfer function, $G(p)$, is separated into $g_1(p) = e^{-\delta p}$ and $g_2(p) =$ all remaining terms in $G(p)$, then as the complex variable, $p = \lambda + i\omega$, is made to take the contour enclosing the positive half of the p -plane, stability can be conveniently determined if the $g_2(p)$ curve lies completely clear of the unit circle, $g_1(p)$. A Nyquist Diagram of the denominator of $g_2(p)$ also is required to determine if there are any poles in the positive half plane.

For an unstable case in which $g_2(p)$ does intersect the unit circle, $g_1(p)$, stability can be insured by designing a feedback

circuit transfer function which will cause the $g_2(p)$ curve to move clear of the $g_1(p)$ curve, and still meet the requirements of the Nyquist Diagram concerning poles in the positive half plane.

For a bipropellant rocket the temperature of the combustion gases is a function of the local mixture ratio. As the mixture ratio operates away from the steady-state value, \bar{r} , the fractional variation of the temperature varies as:

$$\frac{T_g - \bar{T}_g}{\bar{T}_g} = 2K \frac{r - \bar{r}}{\bar{r}} \quad \text{or,} \quad K = \frac{1}{2} \frac{\bar{r}}{\bar{T}_g} \frac{dT_g}{dr}$$

This defines K which turns out to be an interesting parameter of the system. K may be either positive or negative, although, as pointed out by L. Crocco, K is generally positive.

II. DEVELOPMENT OF EQUATIONS

Under the assumptions given above, the equation of the combustion chamber for a bipropellant rocket was developed by L. Crocco: (See Figure 1 for schematic diagram of system).

$$\frac{d\phi}{dz} + 2K[(\mu_o - \mu_f)_{\delta+1} - (\mu_o - \mu_f)_{\delta}] + \phi - K(\mu_o - \mu_f)_{\delta+1} =$$

$$(\frac{1}{2} + H)\mu_o/\delta + (\frac{1}{2} - H)\mu_f/\delta + \eta(\phi - \phi/\delta) \quad (2)$$

Following H. S. Tsien and considering the propellant to be fed by a centrifugal pump run at constant speed the following equations for the bipropellant feed system are developed:

$$-\frac{1}{\alpha}(P_o + \frac{1}{2})(\mu_o + \frac{dK_o}{dz}) - P_o\phi = \mu_o + J_o \frac{d}{dz}(\mu_o + \frac{dK_o}{dz}) \quad (3)$$

$$-\frac{1}{\alpha}(P_f + \frac{1}{2})(\mu_f + \frac{dK_f}{dz}) - P_f\phi = \mu_f + J_f \frac{d}{dz}(\mu_f + \frac{dK_f}{dz}) \quad (4)$$

Equations (2), (3) and (4) specify the transient behavior of the fuel and oxidizer supply systems coupled with the combustion chamber when the reservoir capacity in the feed line, K_o and K_f , are specified. The closed loop stabilization circuit can be completed by requiring K_o and K_f to be a function of ϕ . This means that the reservoir capacity responds to pressures from the

combustion chamber through a suitable amplifier and servo system.

Thus K_0 and K_f are assumed to satisfy a pair of integro-differential equations,

$$T_0 \left(\frac{d}{dz} \right) \phi = K_0 \quad (5)$$

$$T_f \left(\frac{d}{dz} \right) \phi = K_f \quad (6)$$

where T_f and T_0 correspond to a ratio of functions (generally polynomials) in d/dz .

Trying a solution of the form:

$$\begin{aligned} \phi &= A' e^{pz} & u_0 &= B' e^{pz} & u_f &= D' e^{pz} \\ K_0 &= L' e^{pz} & K_f &= M' e^{pz} \end{aligned} \quad (7)$$

where now $p = \lambda + i\omega$ is complex, as are A' , B' , D' , L' and M' .

Eliminating the common factor e^{pz} , equations (2), (3), (4), (5) and (6) represent a solution of the system if the five homogeneous first degree equations below are simultaneously satisfied:

$$(1 - n + p + ne^{-p\delta})A' - (g + \frac{1}{2})e^{-p\delta}B' + (g - \frac{1}{2})e^{-p\delta}D' = 0 \quad (8)$$

$$P_0 A' + \left[1 + \frac{1}{\alpha}(P_0 + \frac{1}{2}) + J_0 p \right] B' + \left[\frac{1}{\alpha}(P_0 + \frac{1}{2})p + J_0 p^2 \right] L' = 0 \quad (9)$$

$$P_f A' + \left[1 + \frac{1}{\alpha}(P_f + \frac{1}{2}) + J_f p \right] D' + \left[\frac{1}{\alpha}(P_f + \frac{1}{2})p + J_f p^2 \right] M' = 0 \quad (10)$$

$$F_0(p) A' - L' = 0 \quad (11)$$

$$F_f(p) A' - H' = 0 \quad (12)$$

Since they are homogeneous equations, they can be simultaneously satisfied if, and only if, the following determinant of the coefficients of the above equations vanishes:

$$\begin{vmatrix} p + (1-n) + ne^{-\delta p} & -(g+\frac{1}{2})e^{-\delta p} & (g-\frac{1}{2})e^{-\delta p} & 0 & 0 \\ P_0 & [1 + \frac{1}{\alpha}(P_0 + \frac{1}{2}) + J_0 p] & 0 & [\frac{1}{\alpha}(P_0 + \frac{1}{2})p + J_0 p^2] & 0 \\ P_f & 0 & [1 + \frac{1}{\alpha}(P_f + \frac{1}{2}) + J_f p] & 0 & [\frac{1}{\alpha}(P_f + \frac{1}{2})p + J_f p^2] \\ F_0(p) & 0 & 0 & -1 & 0 \\ F_f(p) & 0 & 0 & 0 & -1 \end{vmatrix}$$

where $g = H + 2K - Ke^{-p}$ has been used for convenience.

Expanding the determinant gives equation (14) below; if p satisfies this equation, our assumed solution, equation (7), will be a possible solution of the system.

$$\begin{aligned}
 & [p + (q-n)][1 + \frac{1}{\alpha}(P_f + \frac{1}{2}) + J_f p][1 + \frac{1}{\alpha}(P_0 + \frac{1}{2}) + J_0 p] + \\
 & e^{-\delta p} \left\{ n[1 + \frac{1}{\alpha}(P_f + \frac{1}{2})][1 + \frac{1}{\alpha}(P_0 + \frac{1}{2})] + P_0(q + \frac{1}{2})[1 + \frac{1}{\alpha}(P_f + \frac{1}{2})] + \right. \\
 & \left. - P_f(q - \frac{1}{2})[1 + \frac{1}{\alpha}(P_0 + \frac{1}{2})] \right\} + p e^{-\delta p} \left\{ n J_f [1 + \frac{1}{\alpha}(P_0 + \frac{1}{2})] + \right. \\
 & \left. n J_0 [1 + \frac{1}{\alpha}(P_f + \frac{1}{2})] - J_0 P_f(q - \frac{1}{2}) + J_f P_0(q + \frac{1}{2}) \right\} + p^2 e^{-\delta p} n J_0 J_f + \\
 & p e^{-\delta p} F_f(p) \left\{ [q - \frac{1}{2}][\frac{1}{\alpha}(P_f + \frac{1}{2})][1 + \frac{1}{\alpha}(P_0 + \frac{1}{2})] \right\} + \\
 & p^2 e^{-\delta p} F_f(p) (q - \frac{1}{2}) \left\{ [\frac{1}{\alpha}(P_f + \frac{1}{2})][J_0] + J_f [1 + \frac{1}{\alpha}(P_0 + \frac{1}{2})] \right\} + \\
 & p^3 e^{-\delta p} F_f(p) (q - \frac{1}{2})(J_f J_0) + \\
 & p e^{-\delta p} F_0(p) \left\{ [q + \frac{1}{2}][\frac{1}{\alpha}(P_0 + \frac{1}{2})][1 + \frac{1}{\alpha}(P_f + \frac{1}{2})] \right\} + \\
 & p^2 e^{-\delta p} F_0(p) (q + \frac{1}{2}) \left\{ [\frac{1}{\alpha}(P_0 + \frac{1}{2})][J_f] + J_0 [1 + \frac{1}{\alpha}(P_f + \frac{1}{2})] \right\} + \\
 & p^3 e^{-\delta p} F_0(p) (q + \frac{1}{2})(J_0 J_f) = G(p) = 0 \quad (14)
 \end{aligned}$$

For the system to be stable, the roots p of equation (14) should not have real parts. The problem of stabilizing the rocket motor thus becomes one of designing the closed loop transfer function, $F_0(p) + F_f(p)$, so that this criterion is satisfied. This condition can be investigated most easily by use of the Tsien-Satche Diagram and a Nyquist Diagram.

If the complex variable p is made to take a contour as in Figure 2 enclosing the positive half of the p -plane from $-\infty$ to $+\infty$ and around a circle in the positive direction with infinite radius, each root of $G(p) = 0$ (equation 14) in the positive half plane will cause $G(p)$ to make a complete revolution about the origin. Separating $G(p)$ into two parts, $g_1(p)$ and $g_2(p)$, by dividing by the coefficient of the exponential term, $e^{-\delta p}$, gives:

$$G(p) = g_1(p) - g_2(p)$$

$$= e^{-\delta p} - \left\{ \frac{[p + 1 - \eta][A + J_f p][B + J_o p]}{[n I_o J_f p^2 + (D + S e^{-\delta p})p + (C + R e^{-\delta p}) + F_o(p)L + F_f(p)M]} \right\} \quad (15)$$

where

$$A \equiv 1 + \frac{1}{\alpha} (P_f + \frac{1}{2}) \quad (16)$$

$$B \equiv 1 + \frac{1}{\alpha} (P_0 + \frac{1}{2}) \quad (17)$$

$$C \equiv n + (P_0 + P_f) (\frac{1}{2} + \frac{1}{4\alpha} + \frac{n}{\alpha} + \frac{n}{2\alpha}) + (P_0 - P_f) (H + 2K + \frac{H}{2\alpha} + \frac{K}{\alpha}) + \\ P_0 P_f (\frac{1}{\alpha} + \frac{n}{\alpha^2}) + \frac{n}{\alpha} (1 + \frac{1}{4\alpha}) \quad (18)$$

$$D \equiv [(J_f + J_0) (n + \frac{n}{2\alpha}) + (J_f P_0 + J_0 P_f) (\frac{1}{2} + \frac{n}{\alpha}) + (J_f P_0 - J_0 P_f) (H + 2K)] \quad (19)$$

$$E \equiv (P_f - P_0) (K + \frac{K}{\alpha}) \quad (20)$$

$$S \equiv -K (J_f P_0 - J_0 P_f) \quad (21)$$

$$H \equiv \left\{ (H + 2K - \frac{1}{2}) \left[(A - 1) (B_p + J_0 p^2) + J_f (B_p^2) + \right. \right. \\ \left. J_f J_0 p^3 \right] - K e^{-D} \left[(A - 1) (B_p + J_0 p^2) + J_f (B_p^2) + J_f J_0 p^3 \right] \right\} \quad (22)$$

$$L \equiv \left\{ (H + 2K + \frac{1}{2}) \left[(B - 1) (A_p + J_f p^2) + J_0 (A_p^2) + J_f J_0 p^3 \right] + \right. \\ \left. - K e^{-D} \left[(B - 1) (A_p + J_f p^2) + J_0 (A_p^2) + J_f J_0 p^3 \right] \right\} \quad (23)$$

Note that in these definitions, A, B, C, D, R, S, are constants of the system, but that L and M include the variable (p).

With this arrangement of terms, $G(p)$ becomes a vector with vertex on $g_1(p)$ and the starting point on $g_2(p)$. As p makes the stated contour of Figure 2, $g_1(p)$ becomes a unit circle and $g_2(p)$ prescribes various contours dependent on its form.

It is also necessary to investigate the coefficient of $e^{-\delta p}$ (this is the denominator of $g_2(p)$ as written in equation (15) to ascertain if it has any poles or zeros in the positive half plane.

If the coefficient of $e^{-\delta p}$ has s poles and r zeros in the right half p -plane, then as p traces a clockwise contour as in Figure 2, the coefficient will trace $r-s$ clockwise revolutions. Therefore, for stability $g_2(p)$ must make r counterclockwise revolutions around the unit circle. Thus even though the primary condition of stability is that $g_2(p)$ lie completely clear of the unit circle, $g_1(p)$, it must also satisfy the conditions dictated by the number of poles in the positive half plane of the coefficient of the exponential term, $e^{-\delta p}$.

III. STABILITY OF BIROMILLANT SYSTEMS WITHOUT FEEDBACK

To investigate first the coupled feed system and combustion chamber without the feedback circuit, set $K_o(p)$ and $K_f(p)$ equal to zero. This reduces equation (15) to:

$$G(p) = e^{-\delta p} \left\{ \frac{[p+1-n][A+J_f p][B+J_o p]}{-[nJ_o J_f p^2 + (D+Se^{-p})p + C+Re^{-p}]} \right\} \quad (24)$$

where the constants A, B, C, D, S and R are defined in equations (16) through (21).

CASE I: (Stable Case, $K = 0.2$)

Let $n = 0.1$; $\alpha = 1.0$; $\bar{r} = 2.75$; $R = 0.233$; $T_g = 4500^\circ K$;

$dT_g/dr = 650$; $K = 0.2$; $J_o = 4.0$; $J_f = 0.8$; $P_o = 0.5$;

$P_f = 1.0$.

Substituting these values into equations (16) through (21) gives:

$A = 2.5$; $B = 2.0$; $C = 1.65$; $D = 1.08$; $R = 0.2$;

$S = 0.72$.

Thus, equation (24) becomes:

$$G(p) = e^{-\delta p} \left\{ \frac{(p+0.9)(2.5+0.8p)(2.0+4.0p)}{-[0.32p^2 + (1.08+0.72e^{-p})p + (1.65+0.2e^{-p})]} \right\} \quad (25)$$

Now let $p = i\omega$, where ω is the reduced angular frequency.

Equation (25) reduces to:

$$G(p) = e^{-i\delta\omega} - \left\{ \frac{(-3.2\omega^3 + 15.44\omega)i - 14.48\omega^2 + 4.5}{-[-0.32\omega^2 + (1.08 + 0.72e^{-i\omega})i\omega + (1.65 + 0.2e^{-i\omega})]} \right\} \quad (26)$$

Substituting values for ω gives the Tsien-Satche Diagram for $g_2(p)$ plotted in Figure 3. Checking the denominator of $g_2(p)$ for poles gives the Nyquist Diagram plotted in Figure 4. The numerator is plotted in Figure 5.

From the figures it is evident that this case is stable since the $g_2(p)$ curve is completely clear of the unit circle and makes no loops about it. Also, the denominator in the Nyquist Diagram is proven not to have any zeros in the positive half p -plane, since it does not make any revolutions about the origin.

CASE II: (Stable Case, $K = 0.3$).

Let $n = 0.1$; $\alpha = 1.0$; $\bar{P} = 2.75$; $H = 0.233$; $T_g = 4500^\circ K$;
 $dT_g/dr = 1000$; $K = .3$; $J_0 = 4.0$; $J_f = 0.8$; $P_0 = 0.5$;
 $P_f = 1.0$.

Substituting these values into equations (16) through (21) gives:

$A = 2.5$; $B = 2.0$; $C = 1.50$; $D = 0.36$; $R = 0.3$; $S = 1.08$.

Letting $p = i\omega$ and substituting these values into equation (24) gives:

$$G(p) = e^{-i\delta\omega} - \left\{ \frac{(-3.2\omega^3 + 15.44\omega)i - 14.48\omega^2 + 4.5}{-[0.32\omega^2 + (0.36 + 1.08e^{-i\omega})i\omega + (15 + 0.3e^{-i\omega})]} \right\} \quad (27)$$

Again, substituting values for ω gives the Tsien-Satche Diagram for $g_2(p)$ plotted in Figure 6; the Nyquist Diagram of the denominator is plotted in Figure 7. The numerator is the same as in Case I (Figure 5).

Changing K in this second case has resulted in a radical change in the Tsien-Satche Diagram. The curve $g_2(p)$ now makes two counter-clockwise loops about the unit circle, although it does not intersect the curve $g_1(p)$. Nevertheless, this is still a stable case since the denominator of $g_2(p)$ makes two clockwise revolutions about the origin in the Nyquist Diagram.

CASE III: (Unstable Case, $K = 0.2$)

Let $n = 0.5$; $\alpha = 1.0$; $\bar{r} = 2.75$; $H = 0.233$; $T_g = 4500^\circ K$;
 $dT_g/dr = 650$; $K = 0.2$; $J_0 = 4.0$; $J_f = 0.8$; $P_0 = 0.5$;
 $\Gamma_f = 1.0$.

Substituting these values into equations (16) through (21) gives:

$A = 2.5$; $B = 2.0$; $C = 3.65$; $D = 5.72$; $E = 0.2$;

$S = 0.72$.

Letting $p = i\omega$ and substituting these values into equation (34) gives:

$$G(p) = e^{-i\omega\tau} - \left\{ \frac{(-3.2\omega^3 + 10.8\omega)i - 13.2\omega^2 + 2.5}{-[-1.6\omega^2 + (5.72 + 0.72e^{-i\omega\tau})i\omega + (3.65 + 0.2e^{-i\omega\tau})]} \right\} \quad (28)$$

Substituting values for ω and plotting gives the Nyquist-Satche Diagram of Figure 8 for $g_2(p)$. The behavior of the denominator of $g_2(p)$ is shown in the plot of Figure 9. The numerator is plotted in Figure 10.

Inspecting the figures it is seen that the $g_2(p)$ curve now intersects the unit circle and thus the rocket motor can be unstable for large reduced time lags. This shift to instability is primarily the result of the change in the value of n from 0.1 to 0.5. Thus, " n ", the pressure exponent of pressure dependence of the processes taking place during the time lag, τ , is shown to be an important system parameter.

CASE IV: (Unstable Case, $K = 0.3$)

Let $n = 0.5$; $\alpha = 1.0$; $\bar{r} = 2.75$; $H = 0.233$; $T_g = 4500^\circ\text{E}$;

$dT_g/dr = 1000$; $K = 0.3$; $J_0 = 4.0$; $J_f = 0.8$; $P_0 = 0.5$;

$k_f = 1.0$.

Substituting these values into equations (16) through (21) gives:

$A = 2.5$; $B = 2.0$; $C = 3.50$; $D = 4.50$; $R = 0.3$;

$S = 1.08$.

Letting $p = i \omega$ and substituting these values into equation (24) gives:

$$G(p) = e^{-i\delta\omega} - \left\{ \frac{(-3.2\omega^3 + 10.8\omega)i - 13.2\omega^2 + 2.5}{-[-1.6\omega^2 + (4.5 + 1.08e^{-i\omega})i\omega + (3.5 + 0.3e^{-i\omega})]} \right\} \quad (29)$$

Substituting values for ω and plotting the values of $g_2(p)$ gives the Tsien-Satche Diagram of Figure 11. The Nyquist Diagram of the denominator is plotted in Figure 12 and the numerator, which is the same as in Case III, is plotted in Figure 10.

In this case changing K from 0.2 to 0.3 did not have the spectacular results as in the stable case, although the $g_2(p)$ curve does have a more complicated shape.

IV. STABILIZATION OF A BIPROPELLANT SYSTEM BY A FEEDBACK CIRCUIT

Turning to the problem of stabilizing an unstable burning rocket motor, it is obvious that a feedback transfer function, $F_0(p)L + F_f(p)M$, is required that will move the $g_2(p)$ curve completely clear of the unit circle for small values of ω plus satisfying the requirements of the Nyquist Diagram for all values of ω . Since the $g_2(p)$ curve can only intersect the unit circle in the region of small values of ω , the $e^{-i\omega}$ terms in the denominator of $g_2(p)$ — (equation 15) — can be expanded in a power series of $(i\omega)$ and higher order terms neglected. Also, define a feed system transfer function, $F_0(p)L + F_f(p)M$, as a series in powers of p :

$$F_0(p)L + F_f(p)M \equiv \bar{\Psi}(p) = a_{-1}/p + a_0 + a_1p + a_2p^2 \quad (30)$$

Substituting these two changes into $G(p)$, equation (15), and letting $p = i\omega$ gives:

$$G(p) = e^{-i\delta\omega} - \left\{ \frac{[i\omega + (1-h)][A + J_f(i\omega)][B + J_o(i\omega)]}{-\{nJ_oJ_f(i\omega)^2 + [D + S(1 - i\omega + \frac{(i\omega)^2}{2!} + \dots)]i\omega + C + R(1 - i\omega + \frac{(i\omega)^2}{2!} + \dots) + \bar{\Psi}\}} \right\} \quad (31)$$

Now clear the denominator of $g_2(p)$ of imaginary terms by multiplying both numerator and denominator by the conjugate of the denominator giving:

$$g_2(i\omega) = - \left\{ \frac{\{ [BA(1-n)][nJ_0J_f + \frac{R}{2} - S + a_2] - [D-R+S+a_1][J_0A(1-n) + J_fB(1-n) + BA] \} (i\omega)^2}{\{ 2[nJ_0J_f + \frac{R}{2} - S + a_2][C+R+a_0] - [D-R+S+a_1]^2 \} (i\omega)^2 + [C+R+a_0]^2} + \right. \\ \left. \frac{\{ [J_0A + J_fB + J_fJ_0(1-n)][C+R+a_0] \} (i\omega)^2 + [C+R+a_0][BA(1-n)]}{\{ 2[nJ_0J_f + \frac{R}{2} - S + a_2][C+R+a_0] - [D-R+S+a_1]^2 \} (i\omega)^2 + [C+R+a_0]^2} + \right. \\ \left. \cdot \frac{\{ [J_0A(1-n) + J_fB(1-n) + BA][C+R+a_0] - [D-R+S+a_1][BA(1-n)] \} \omega}{\{ 2[nJ_0J_f + \frac{R}{2} - S + a_2][C+R+a_0] - [D-R+S+a_1]^2 \} (i\omega)^2 + [C+R+a_0]^2} \right\} \quad (32)$$

This is the approximated equation for the $g_2(p)$ term of the system transfer function and holds for small ω only. Terms of order $(1\omega)^3$ and higher order were neglected in this development.

Now it is necessary to specify the shape of the stabilized curve, $g_2(p)$, near the unit circle and derive the values of a_1 , a_0 , a_1 , a_2 that will meet these requirements. Let this stabilized curve be:

$$g_2(p) = W + X(1\omega) + Y(1\omega)^2 + Z(1\omega)^3 \quad (33)$$

Equate this to $g_2(p)$ in equation (31) and clear by multiplying the denominator by equation (33), transposing the numerator terms to the left hand side and collecting even and odd powers of (1ω) together:

$$\left\{ W \left[n J_0 J_f + \frac{R}{2} - S \right] + X [D - R + S] + Y [C + R] + W a_2 + X a_1 + Y a_0 + Z a_{-1} \right\} (i\omega)^2 +$$

$$[J_0 A + J_f B + J_f J_0 (1-n)] (i\omega)^2 + \left\{ W [C + R] + AB(1-n) + W a_0 + X a_{-1} \right\} = 0 \quad (34)$$

$$\left\{ W \left[\frac{S}{2} - \frac{R}{2} \right] + X \left[n J_0 J_f + \frac{R}{2} - S \right] + Y [D - R + S] + Z [C + R] + X a_2 + Y a_1 + Z a_0 \right\} (i\omega)^3 +$$

$$[J_0 J_f] (i\omega)^3 + \left\{ W [D - R + S] + X [C + R] + [J_0 A (1-n) + J_f B (1-n) + BA] + \right. \quad (35)$$

$$\left. W a_1 + X a_0 + Y a_{-1} \right\} (i\omega) + W a_{-1} = 0 \quad (35)$$

Note that in this development terms of order $(i\omega)^4$ and higher were neglected. The coefficient of each $(i\omega)$ term must be independently zero for these equations to be satisfied. Therefore, setting the coefficient of each term, i.e., $(i\omega)^{-1}$, $(i\omega)^0$, $(i\omega)^1$, $(i\omega)^2$ to zero and solving for the unknowns, a_{-1} , a_0 , a_1 , a_2 gives:

$$W a_{-1} = 0$$

$$W a_0 + X a_{-1} = -AB(1-n) - W [C + R]$$

$$W a_1 + X a_0 + Y a_{-1} = -[J_0 A (1-n) + J_f B (1-n) + BA] - W [D - R + S] - X [C + R]$$

$$W a_2 + X a_1 + Y a_0 + Z a_{-1} = -[J_0 A + J_f B + J_f J_0 (1-n)] - W \left[n J_0 J_f + \frac{R}{2} - S \right] + \\ - X [D - R + S] - Y [C + R]$$

These four equations can be solved simultaneously to give explicit relations for a_{-1} , a_0 , a_1 , a_2 in terms of system constants, and thus $F_o(p)L + F_f(p)H$, the feedback system transfer function, is determined.

Solving for the unknown a_{-1} , a_0 , a_1 , a_2 gives:

$$\begin{aligned} a_{-1} &= 0 \\ a_0 &= - \left[\frac{AB}{W} (1-n) \right] - (C + R) \\ a_1 &= - \left[J_o A(1-n) + J_f B(1-n) + BA \right] \frac{1}{W} - (D-R+S) + (C + R) \left(X - \frac{X}{W} \right) + \\ &\quad \left[AB(1-n) \frac{X}{W} \right] \\ a_2 &= + \left[J_o A(1-n) + J_f B(1-n) + BA \right] \left[\frac{X}{W^2} - \frac{1}{W} \right] - \left[nJ_o J_f + \frac{R}{2} - S \right] + \\ &\quad \left[AB(1-n) \right] \left[\frac{X}{W^2} - \frac{X^2}{W^2} \right] - \left[C + R \right] \left[\frac{X^2}{W} - \frac{X^2}{W^2} \right] \end{aligned} \quad (37)$$

For small ω the approximated $g_2(p)$ equation (32) can be used with the feedback transfer function equation (30) to plot the Tsien-Satche Diagram. For large ω the general equation (15) must be used in plotting this diagram; also the Nyquist Diagram of the denominator of $g_2(p)$ must be investigated.

To illustrate the procedure outlined above, consider the unstable case discussed previously where $K = 0.2$. Let the required stabilized curve of $g_2(p)$ be described as follows:



$$g_2(p) = W + X(i\omega) + Y(i\omega)^2 + Z(i\omega)^3 = -2 + 8\omega^2 + 8i\omega. \quad (38)$$

This arbitrary selection of the $g_2(p)$ curve is made to place the stabilized curve in the approximate position of the known stable curves of Cases I and II. Thus, $W = -2$; $X = -8$; $Y = -8$; $Z = 0$. Also, $A = 2.5$; $B = 2.0$; $C = 3.65$; $D = 5.72$; $R = 0.2$; $S = 0.72$ (other values as Case III).

Substituting these values into equation (37) gives: $a_{-1} = 0$; $a_0 = -2.6$; $a_1 = -5.84$; $a_2 = -1.06$. With these values, $\Psi = -2.6 + 1.06\omega^2 - 5.84i\omega$.

Using equation (32) and the above values the following expression is obtained for $g_2(p)$:

$$g_2(p) = - \left\{ \frac{+3.13 - 15.31\omega^2 + i(12.46\omega)}{+1.53 - 3.25\omega^2} \right\} \quad (39)$$

Solving this equation for various values of ω gives the below table of results:

ω	$g_2(p)$	$W + X(i\omega) + Y(i\omega)^2 + Z(i\omega)^3$
0	-2.04	-2.00
$\frac{1}{10}$	-1.98 - i 0.83	-1.92 - i 0.80
$\frac{1}{4}$	-1.56 - i 2.25	-1.5 - i 2.00
$\frac{1}{3}$	-1.22 - i 3.55	-1.12 - i 2.66
$\frac{1}{2}$	+0.97 - i 8.7	0 - i 4.0



This table shows that as ω becomes greater than $1/3$, the values of $g_2(p)$ have too great an error. However, from Figure 13 it is apparent that the curve has been stabilized satisfactorily for small ω .

It is now necessary to investigate the behavior of $g_2(p)$ using the exact equation (15) which includes the feedback circuit; substituting the values determined above into equation (15) results in:

$$G(p) = e^{-sp} \left\{ \frac{-13.2\omega^2 + 2.5 + i(-3.2\omega^3 + 10.8\omega)}{-[-0.54\omega^2 + (0.12 + 0.72e^{-i\omega})i\omega + 1.05 + 0.2e^{-i\omega}]} \right\} \quad (40)$$

Substituting values for ω and plotting $g_2(p)$ gives the Tsien-Satche Diagram of Figure 14. The Nyquist Diagram of the denominator is plotted in Figure 15; the numerator is the same as Case III and is plotted in Figure 10.

From Figure 13 it is evident that the stabilized curve is completely clear of the unit circle for small ω . However, for large ω the addition of the feedback circuit has caused the $g_2(p)$ curve to change in the Tsien-Satche Diagram from no loops about the unit circle in Case III to one with two counterclockwise revolutions about $g_1(p)$ in the stabilized curve of Figure 14. Nevertheless,

the system is still stable since the Nyquist Diagram shows that the denominator of $g_2(p)$ makes two clockwise revolutions about the origin.

Thus an unstable burning rocket motor has been stabilized by an appropriate closed loop feedback system. The circuit chosen to stabilize Case III was a combination of three terms of a differentiating circuit and one term of an integrating circuit. The coefficient of the integrating circuit turned out to be zero indicating this type circuit need not be used.

In order to show the nature of the feedback function, $\Psi(p)$, set $F_F(p) = 0$ and solve for $F_0(p)$ in equation (30).

$$F_0(p) = (a_{-1}/p + a_0 + a_1 p + a_2 p^2) / L \cong A_{-1}/p + A_0 + A_1 p + A_2 p^2 \quad (41)$$

Evaluating L by substituting the values of constants used previously, approximating $e^{-1\omega}$ by a power series in $(i\omega)$ and neglecting higher order terms gives:

$$L = -10.59 (i\omega)^2 - 2.33 (i\omega) \quad (42)$$

Equation (41) can now be evaluated by using the known values of all terms, resulting in:

$$\begin{aligned} F_0(p) &= [-1.06(i\omega)^2 - 5.84(i\omega) - 2.60] / [+10.59(i\omega)^2 + 2.33(i\omega)] \\ &= -1.12 / (i\omega) + 2.57 - 12(i\omega) + 54.77(i\omega)^2 \end{aligned} \quad (43)$$

Therefore, to our order of approximation:



$$\begin{aligned}A_{-1} &= -1.12 \\A_0 &= +2.57 \\A_1 &= -12 \\A_2 &= +54.77\end{aligned}\tag{44}$$

It is now necessary to choose a relationship for $F_0(p)$ that will approach zero for large ω and still retain the desired stabilizing characteristics for small ω . Thus the following expression, which is arbitrarily chosen, describes a circuit that will stabilize the combustion chamber:

$$F_0(p) = (-1.12/p) (1 + B_1p / 1 + B_2p^2 + B_3p^3)\tag{45}$$

To evaluate B_1, B_2, B_3 in terms of the constants in equation (44), equate equation (45) to (43) giving:

$$\begin{aligned}B_1 &= -2.29 \\B_2 &= -10.71 \\B_3 &= +23.9\end{aligned}\tag{46}$$

Thus,

$$F_0(p) = (-1.12/p) (1 - 2.29p / 1 - 10.71p^2 + 23.9p^3)\tag{47}$$

This equation for the closed loop circuit gives the desired stabilization to the rocket motor for low frequency pressure variations in the burning process which could have caused combustion instability.



REFERENCES

1. "Aspects of Combustion Stability in Liquid Propellant Rocket Motors", by L. Grecco, Journal of the American Rocket Society, Vol. 21, 1951, pp 163-178 and Vol. 22, 1952, pp 7-16.
2. "Servo Stabilization of Combustion in Rocket Motors", by H. S. Tsien, to be published July 1952, Journal of the American Rocket Society.
3. "Aerodynamic Stability and Automatic Control", by William Bolloy, Journal of the Aeronautical Sciences, Vol. 18, 1951, pp 569-624.

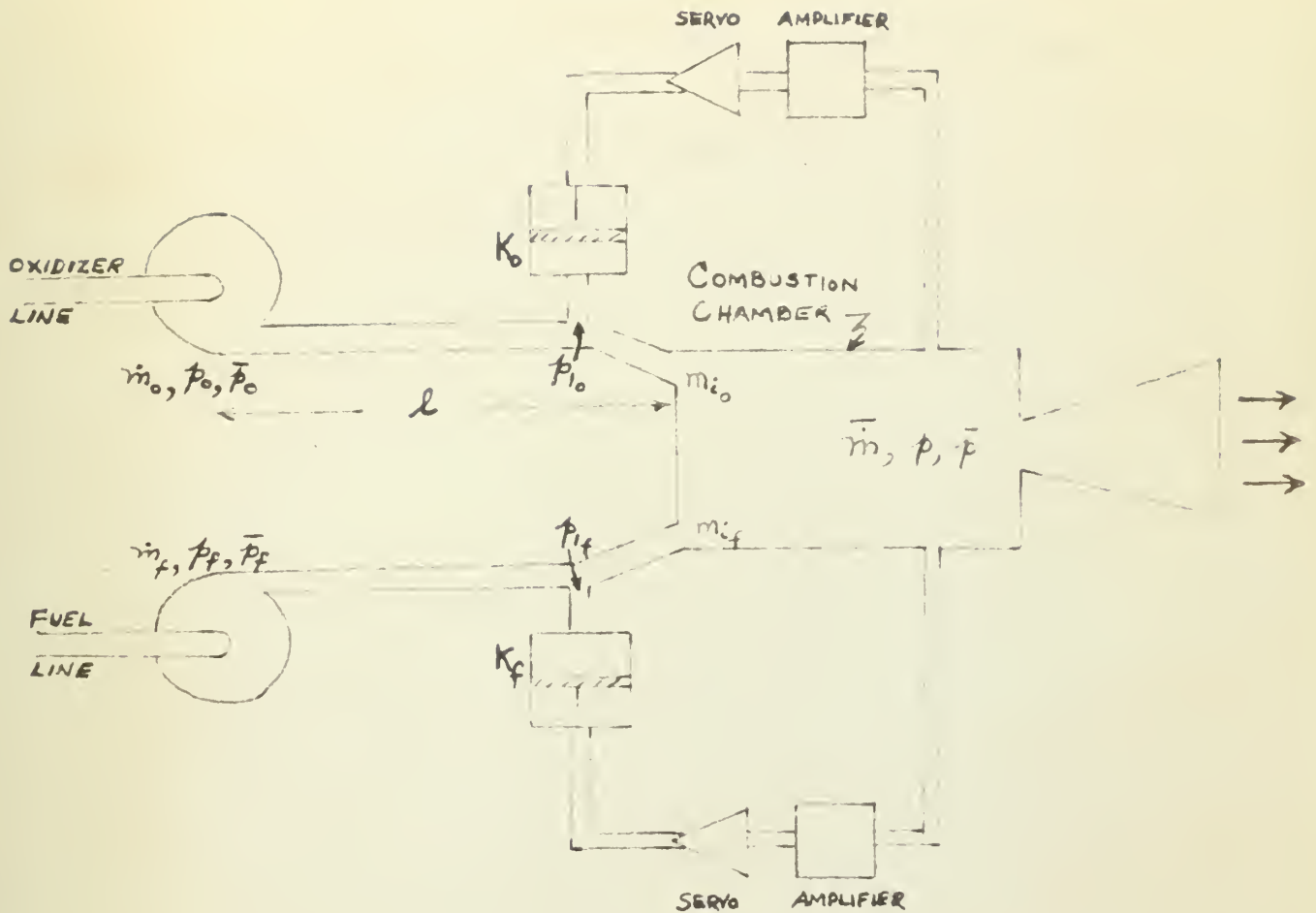


FIGURE 1
SCHEMATIC DIAGRAM OF
FEED SYSTEM, COMBUSTION CHAMBER
AND CLOSED LOOP STABILIZING CIRCUITS
ON OXIDIZER AND FUEL LINES.

FIGURE 2
CONTOUR OF ρ
IN POSITIVE HALF
PLANE

-27-

+i

-i

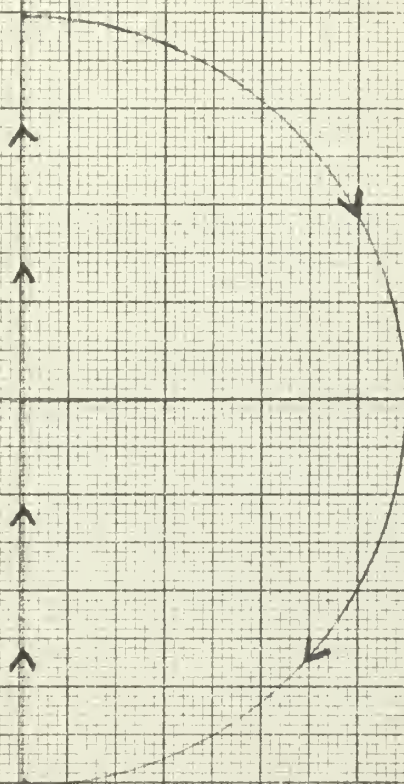
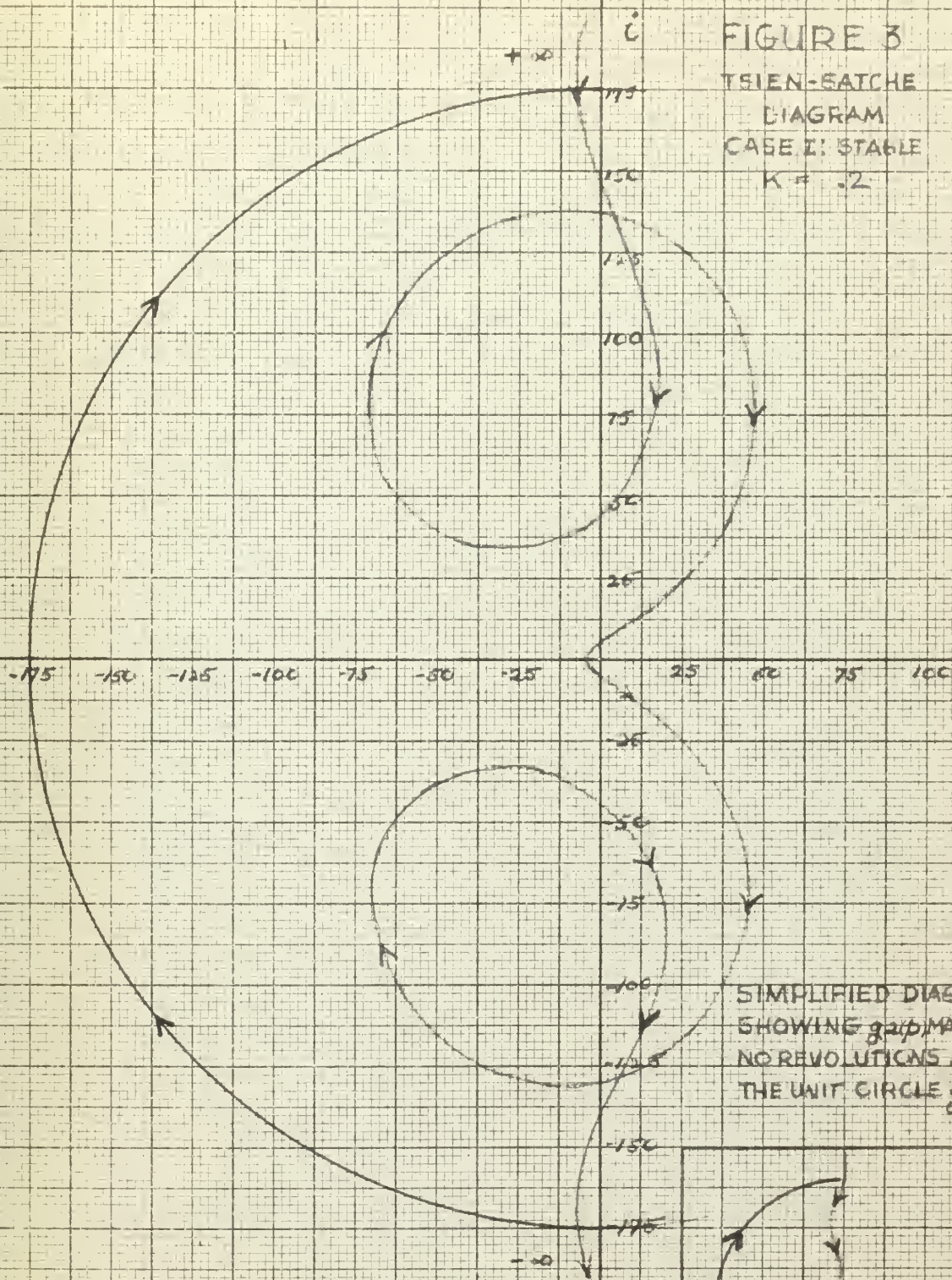


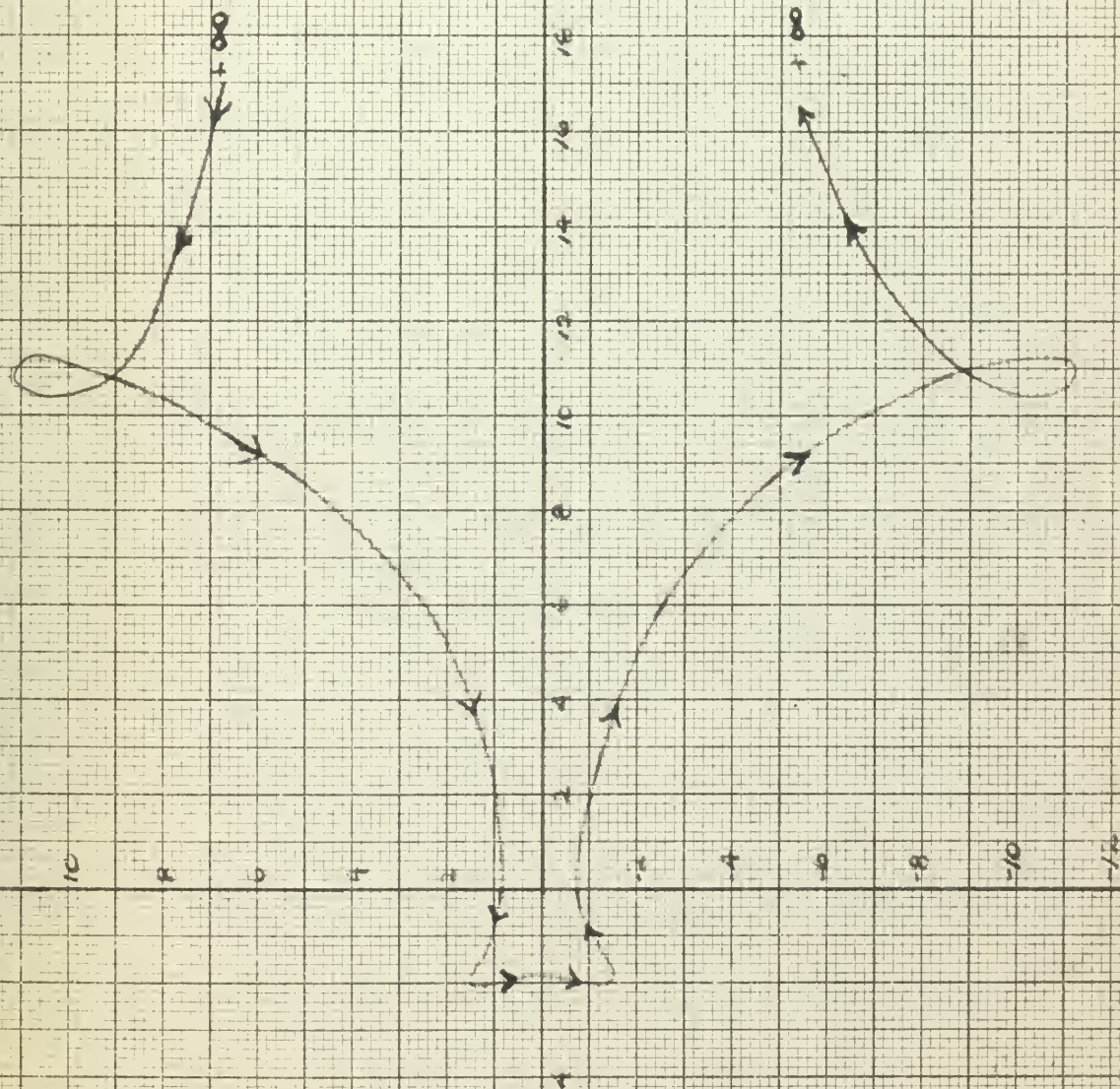
FIGURE 3
TSIEN-SATCHÉ
DIAGRAM
CASE I: STABLE
 $K = .2$



SIMPLIFIED DIAGRAM
SHOWING $g_2(p)$ MAKES
NO REVOLUTIONS ABOUT
THE UNIT CIRCLE $g_1(p)$

FIGURE 4

NYQUIST DIAGRAM FOR
DENOMINATOR OF $g_2(p)$
CASE 1: STABLE; $K = .2$



SIMPLIFIED DIAGRAM SHOWING
DENOMINATOR DOES NOT MAKE
ANY REVOLUTION ABOUT THE ORIGIN

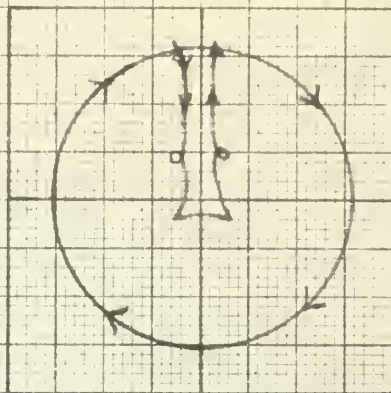


FIGURE 5
PLOT OF NUMERATOR
OF $g_1(p)$ FOR
CASE I AND CASE II

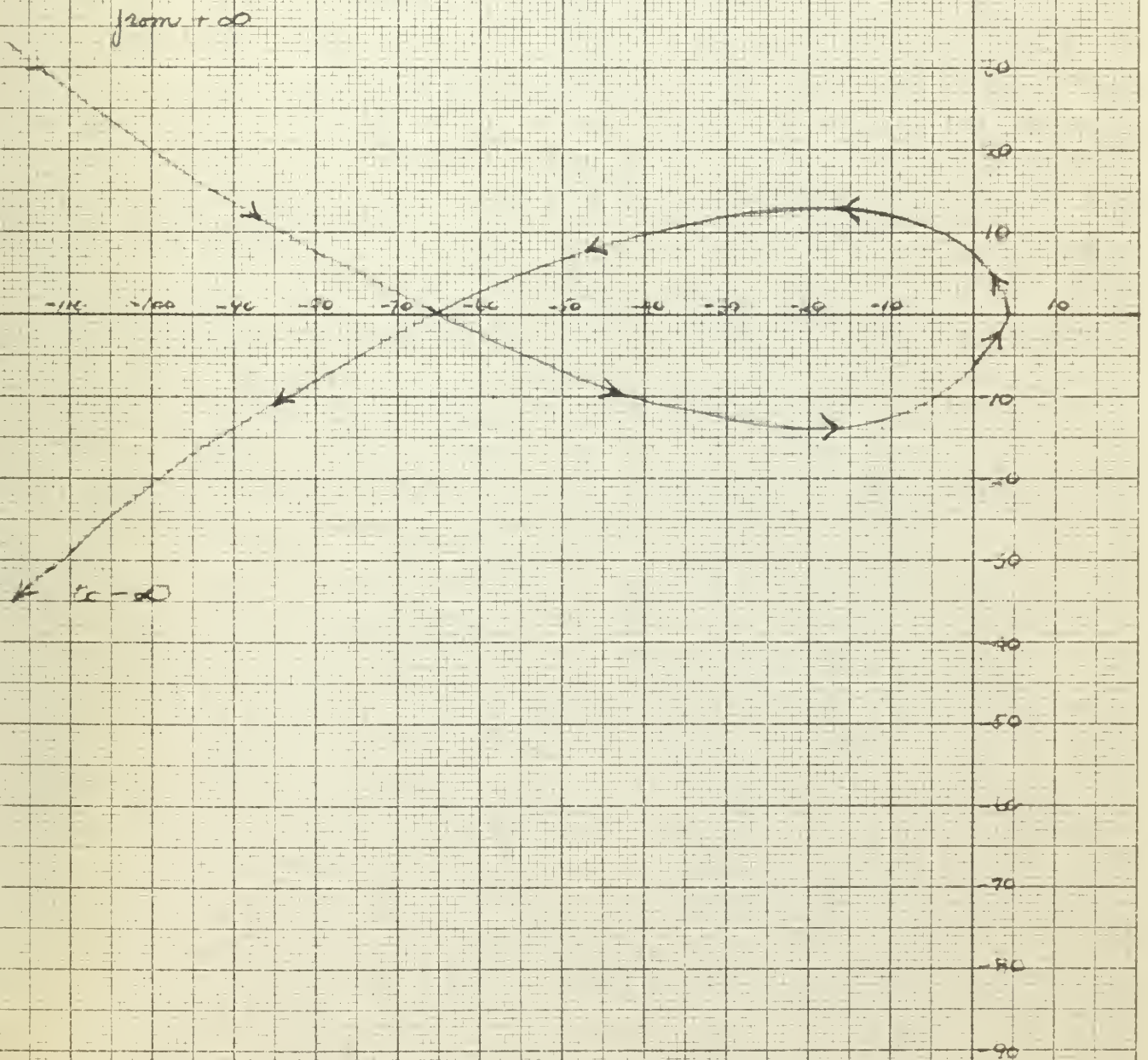


FIGURE 6
TSIEN-SATCHER
DIAGRAM

CASE II: STABLE
 $K = .3$

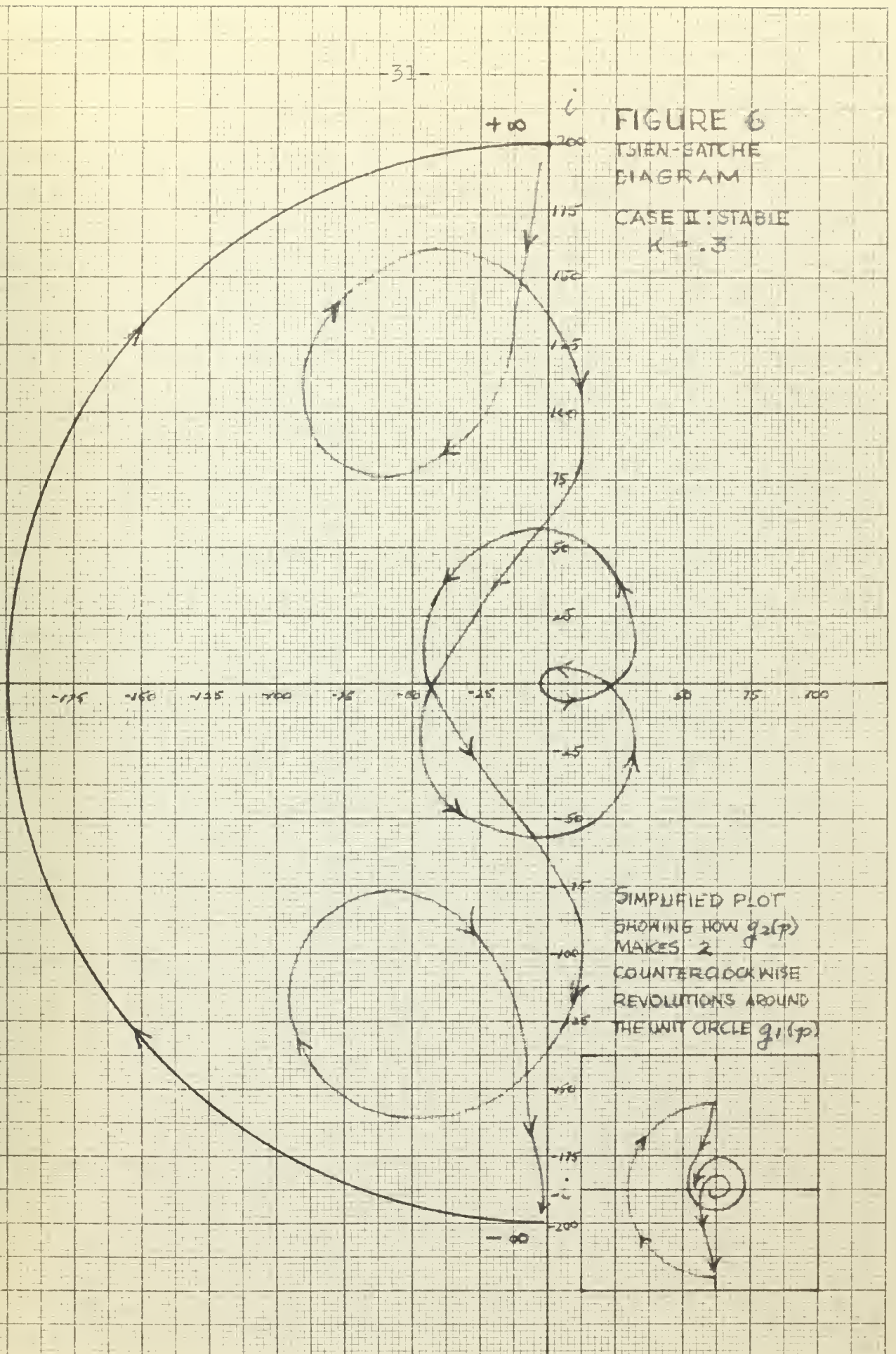
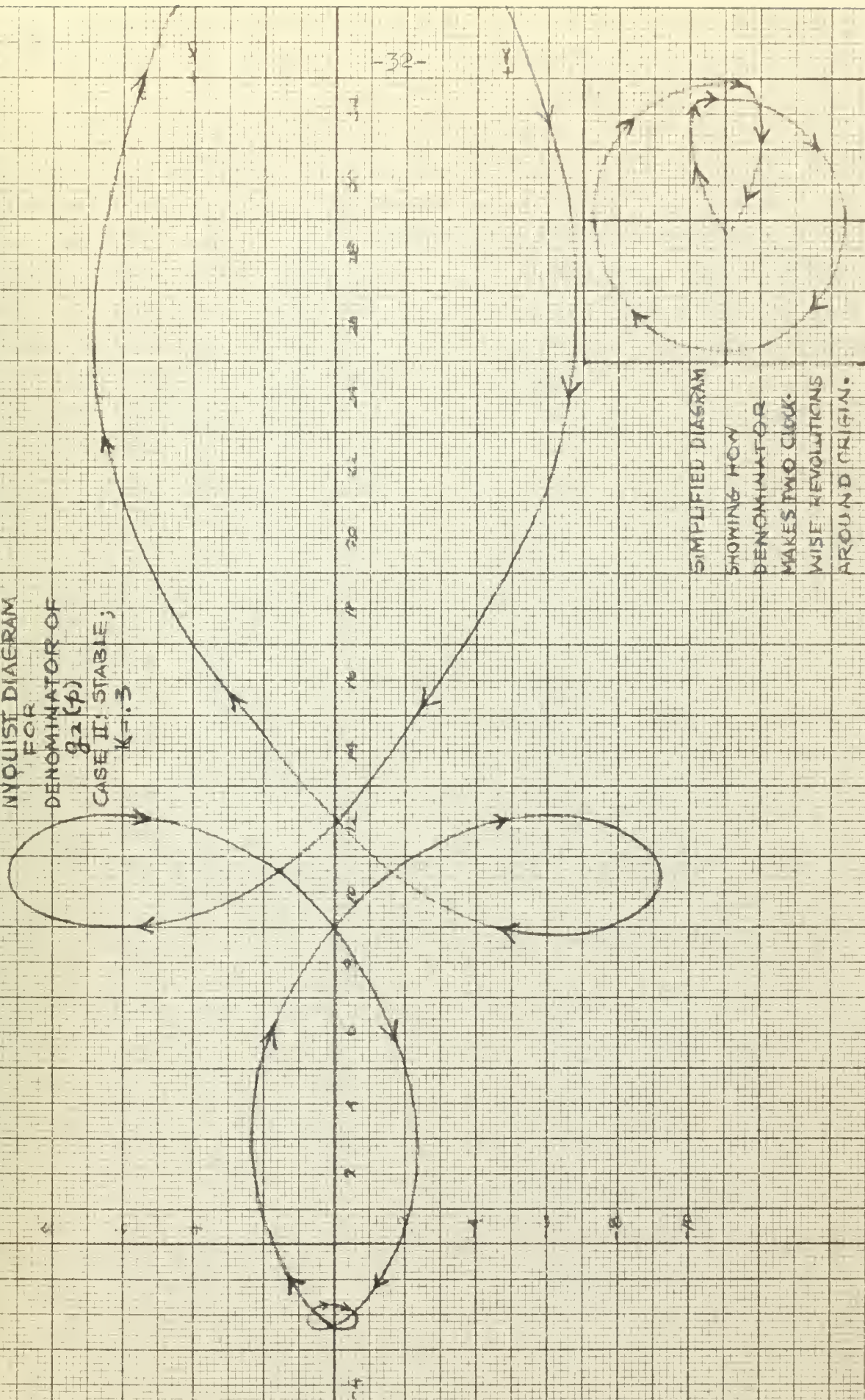


FIGURE 7

NYQUIST DIAGRAM
FOR
DENOMINATOR OF
 $g_2(p)$
CASE II: STABLE;
 $K = 1.3$



-32-

SIMPLIFIED DIAGRAM
SHOWING HOW
DENOMINATOR
MAKES TWO CLOCK-
WISE REVOLUTIONS
AROUND ORIGIN.

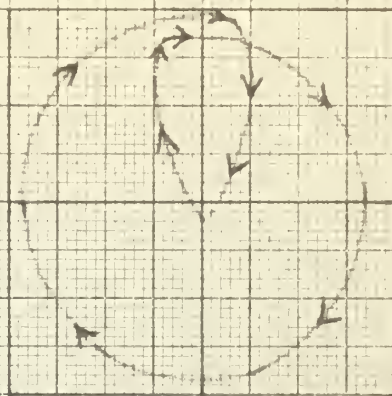




FIGURE 8
TSIEN-SATCHÉ
DIAGRAM FOR CASE III
UNSTABLE $K=0.2$

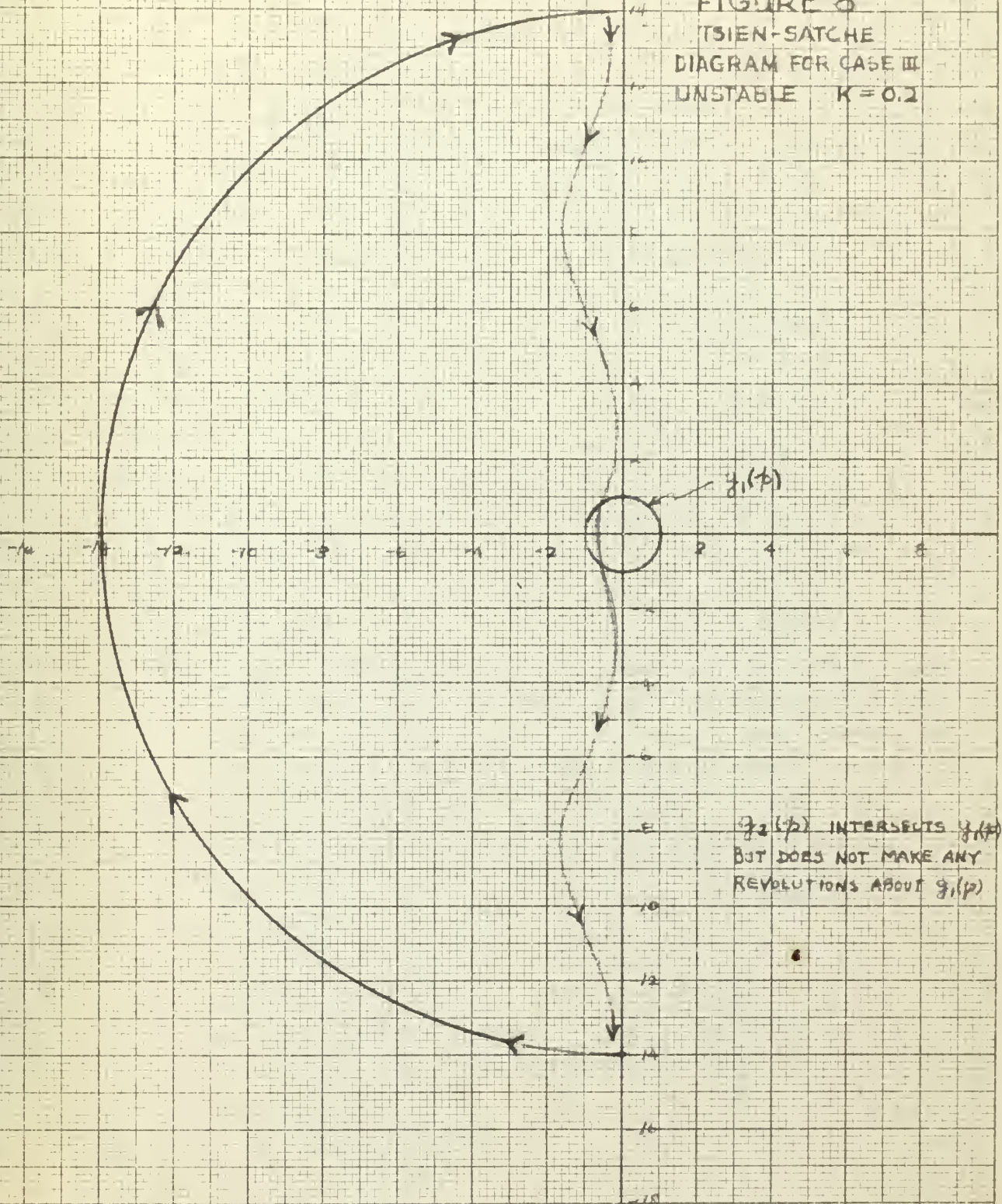
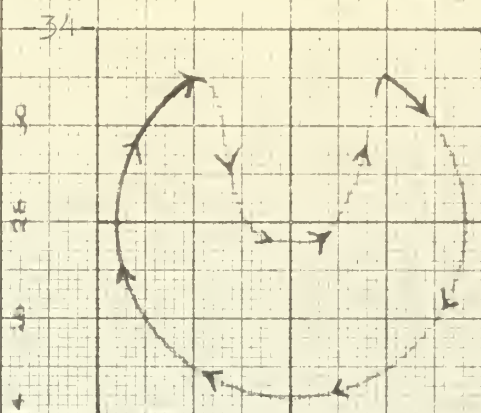
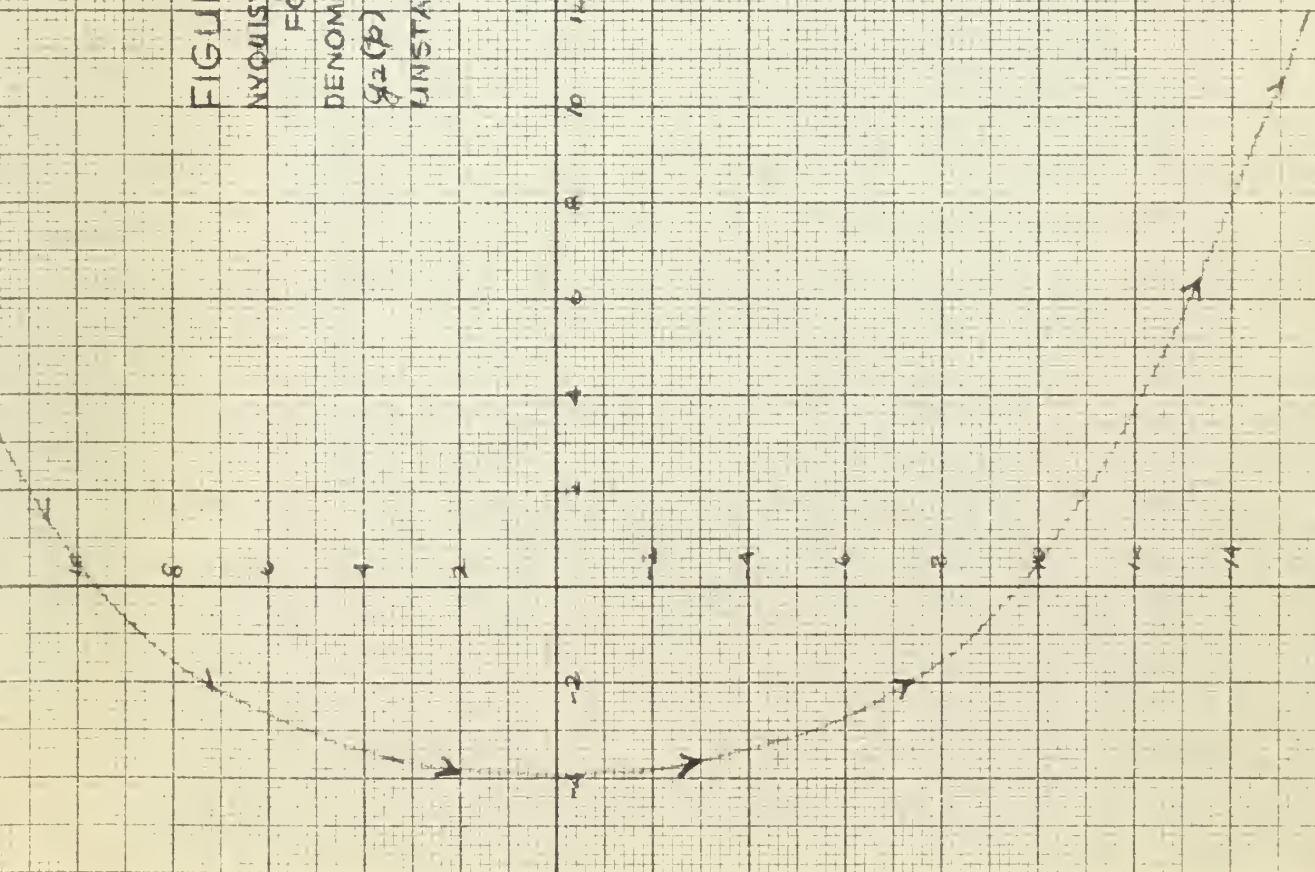
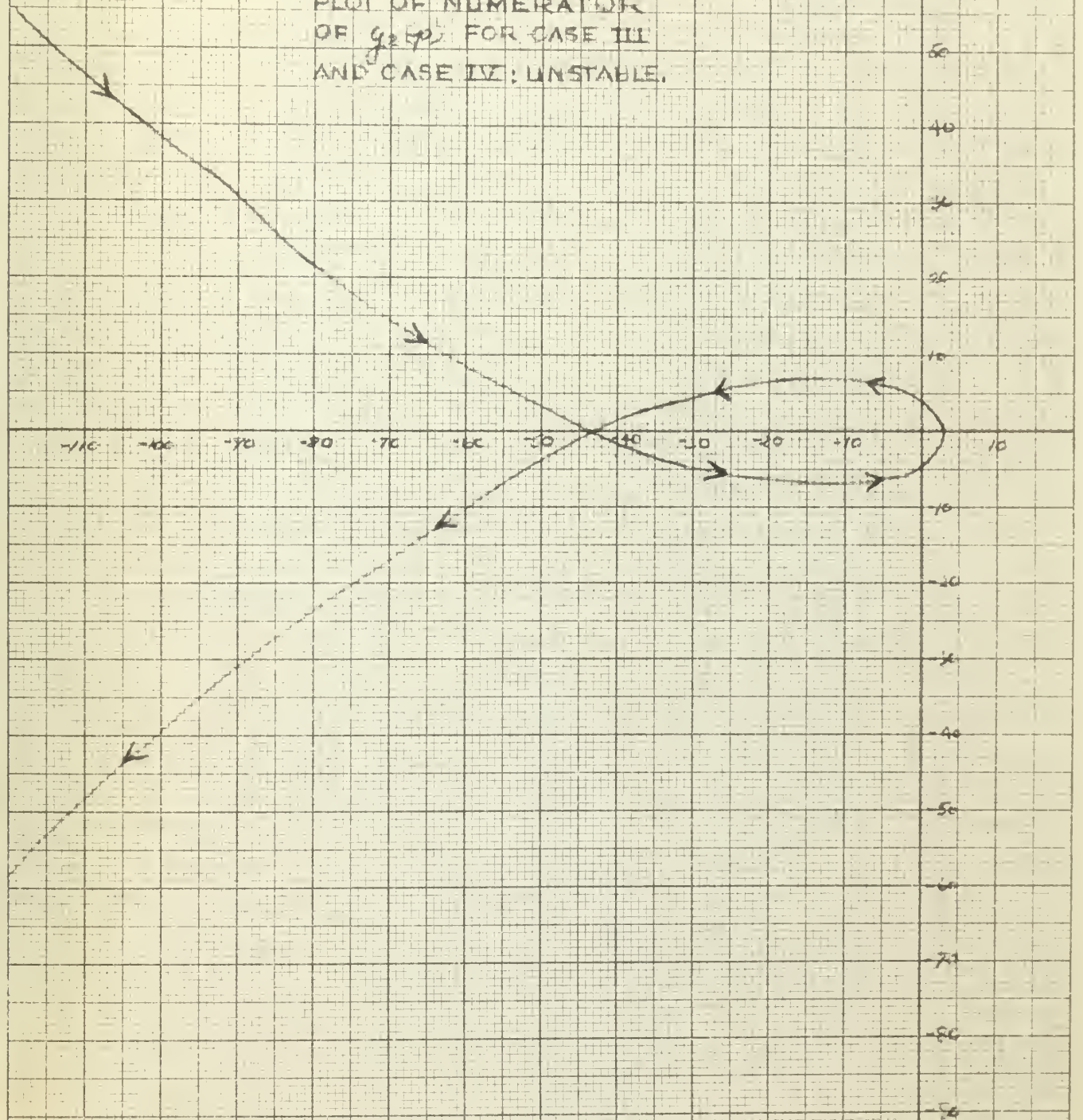


FIGURE 9
 NYQUIST DIAGRAM
 FOR
 DENOMINATOR OF
 $g_2(p)$ CASE III
 UNSTABLE; $K=0.2$



SIMPLIFIED DIAGRAM
 SHOWING
 DENOMINATOR OF $g_2(p)$
 DOES NOT MAKE ANY
 REVOLUTIONS ABOUT THE ORIGIN

FIGURE 10
PLOT OF NUMERATOR
OF $G_2(s)$ FOR CASE III
AND CASE IV: UNSTABLE.



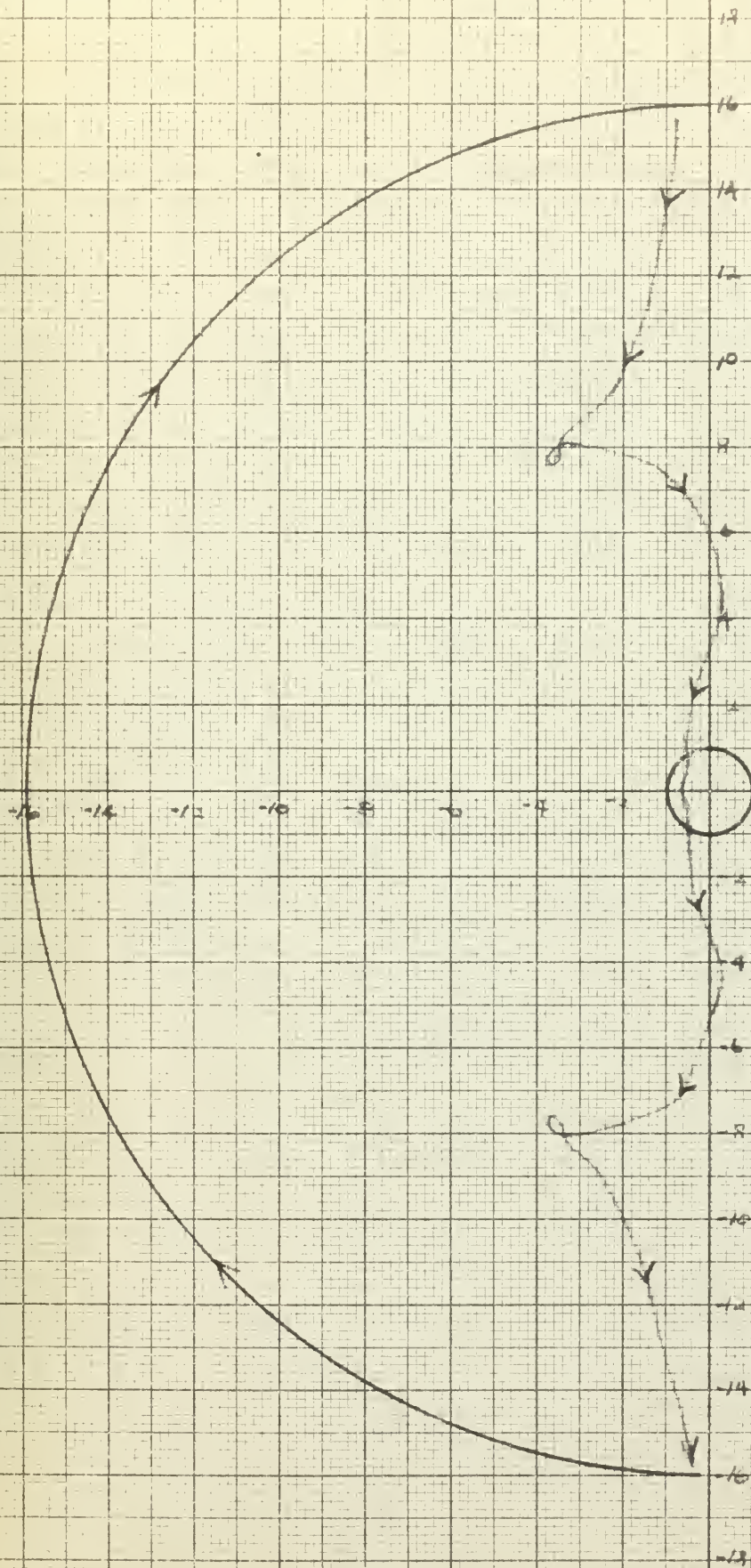


FIGURE 11
TSIEN-SATCHE
DIAGRAM CASE IV
UNSTABLE, $K=0.3$

FIGURE 12
 NYQUIST DIAGRAM OF
 DENOMINATOR OF $g_2(p)$
 CASE IV : UNSTABLE

$K=0.3$

ω

-37-

SIMPLIFIED DIAGRAM

SHOWING DENOMINATOR OF
 $g_2(p)$ DOES NOT MAKE
 ANY REVOLUTIONS ABOUT
 THE ORIGIN.

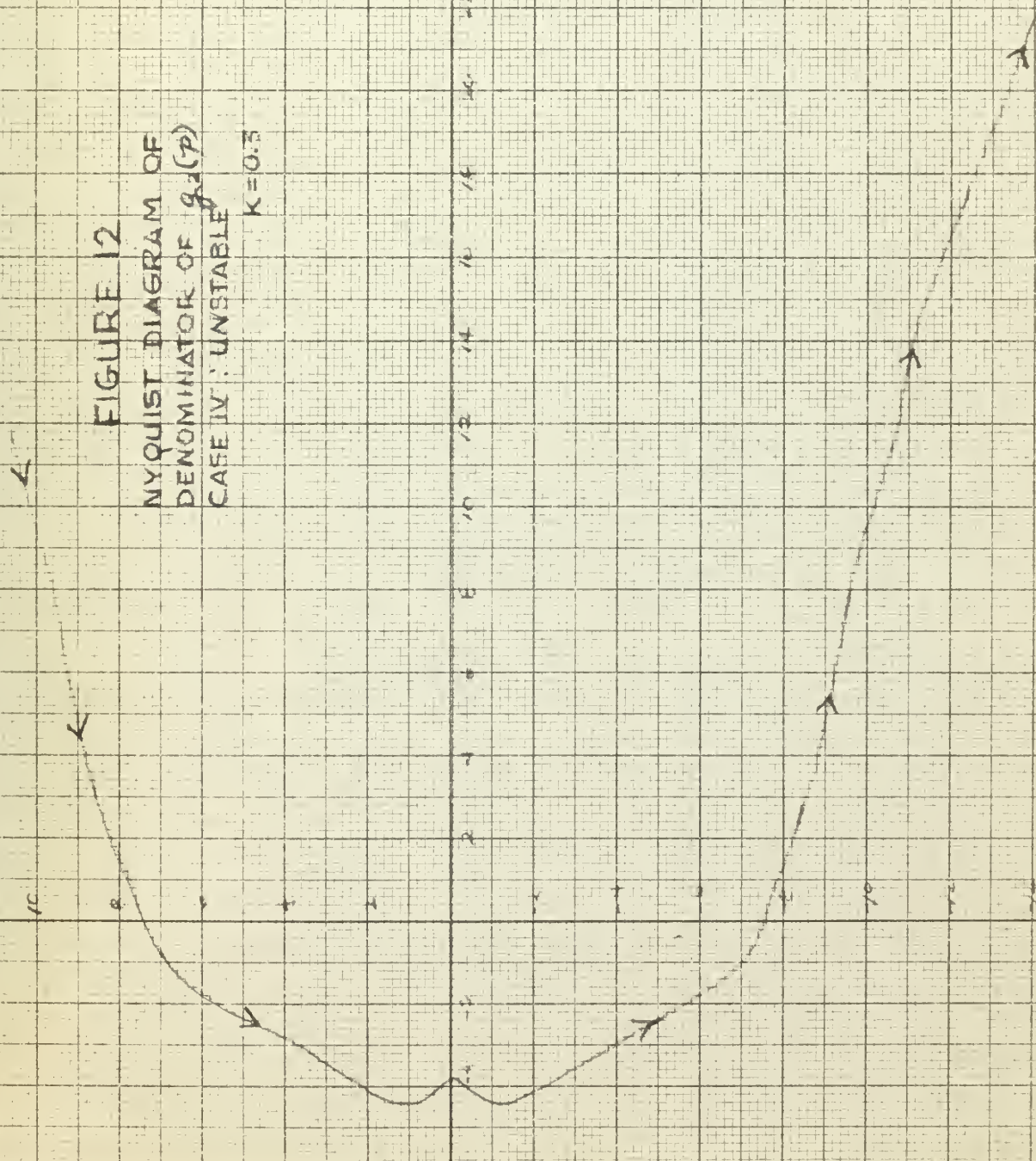
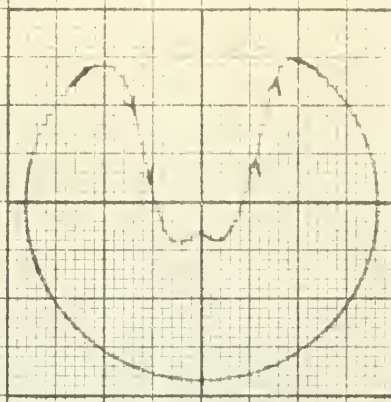


FIGURE 13
 TSIEN-SATCHE DIAGRAMS
 NEAR ORIGIN
 SHOWING BEHAVIOUR OF
 $g_2(p)$ FOR SMALL ω

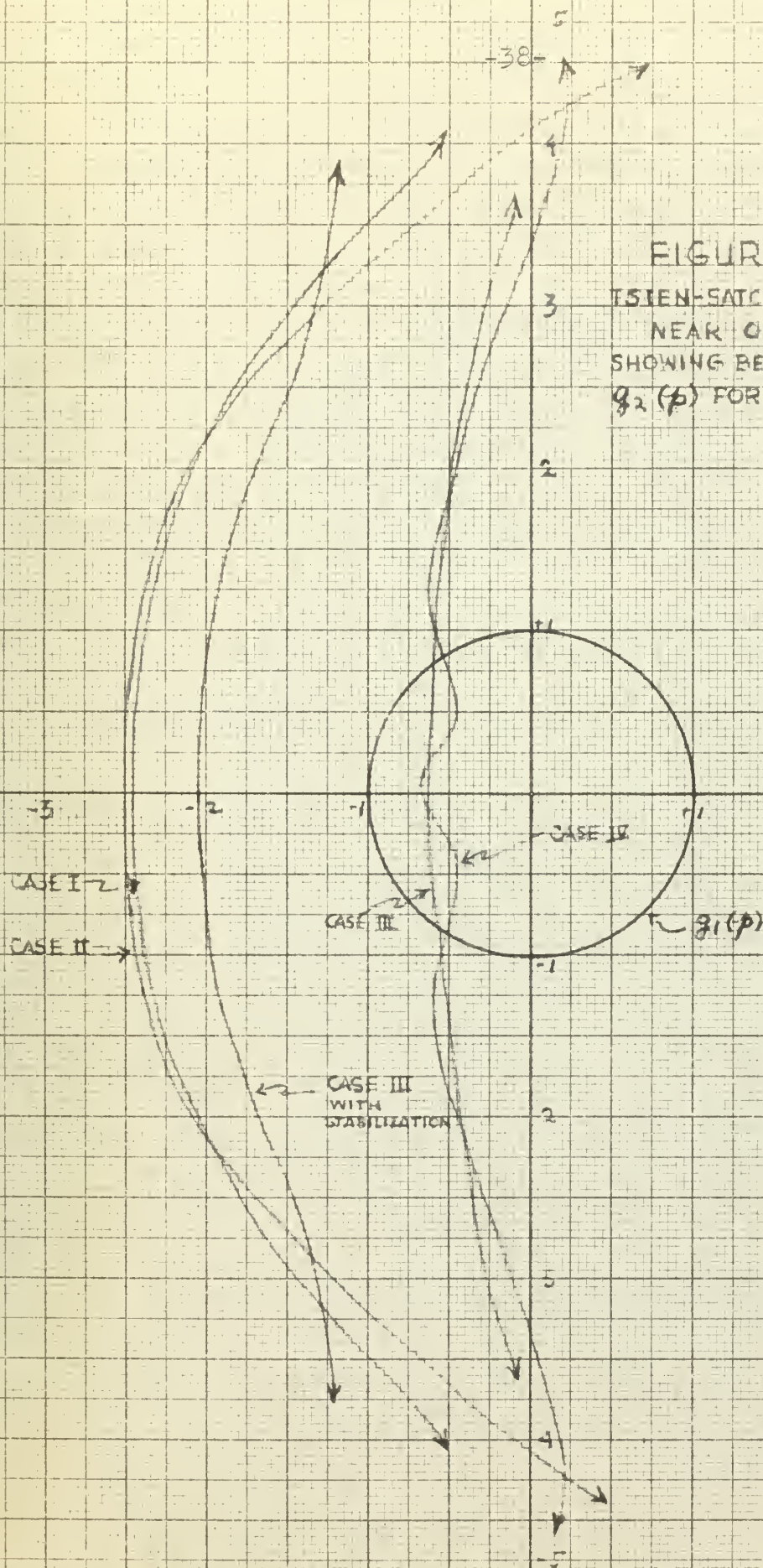


FIGURE 14
TSIEN-SATCHE
DIAGRAM
STABILIZED CASE III

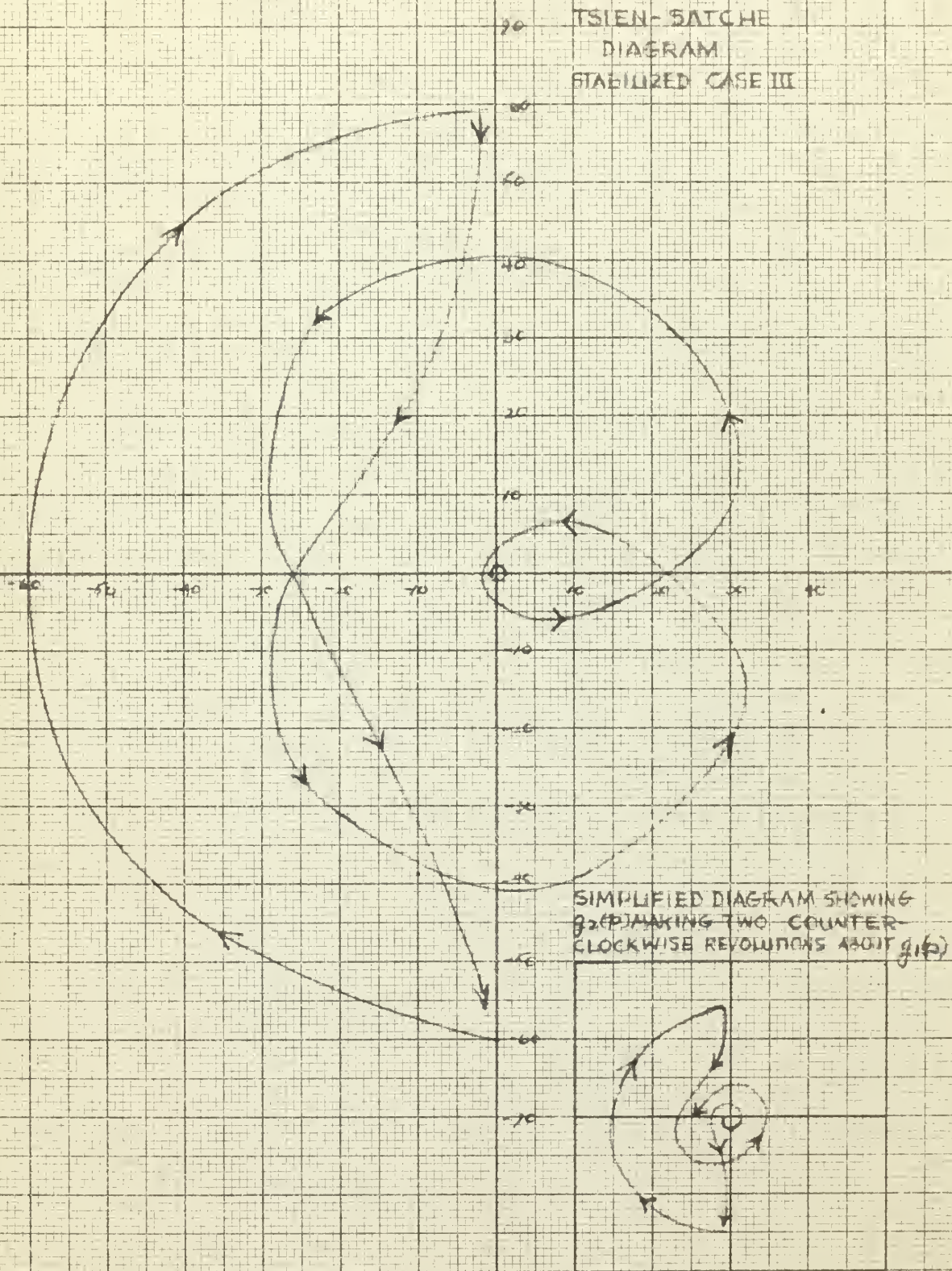
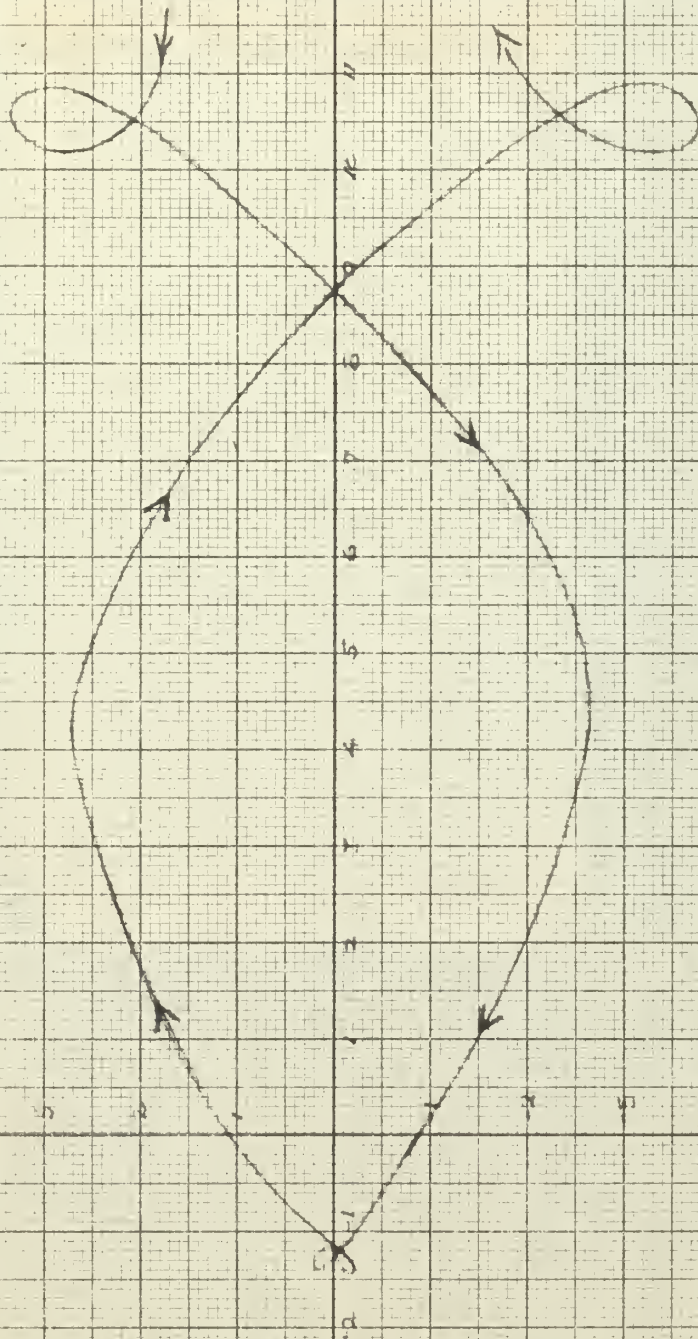
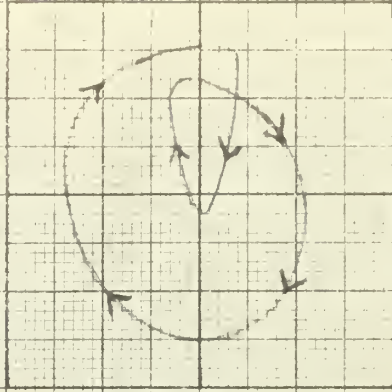


FIGURE 15
 NYQUIST DIAGRAM
 CASE III
 STABILIZED



-40-

SIMPLIFIED DIAGRAM
 SHOWING DENOMINATOR OF
 $G(s)P(s)$ MAKING TWO COUNTER-
 CLOCKWISE REVOLUTIONS AROUND ORIGIN



Date Due

Thesis

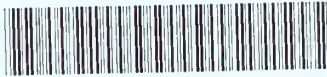
17325

C757 Cox

Stabilization of a
bipropellant liquid
rocket motor.

thesC757

Stabilization of a bipropellant liquid r



3 2768 002 09012 8

DUDLEY KNOX LIBRARY